First seismic record for intra-arc strike-slip tectonics along the Liquine-Ofqui fault zone at the obliquely convergent...

Article *in* Tectonophysics · July 2008

DOI: 10.1016/j.tecto.2008.04.014

CITATIONS
84

READS
231

6 authors, including:

Dietrich Lange
Helmholtz Centre for Ocean Research Kiel
53 PUBLICATIONS **468** CITATIONS
SEE PROFILE

Jose Cembrano
Pontifical Catholic University of Chile
116 PUBLICATIONS **2,145** CITATIONS
SEE PROFILE

Andreas Rietbrock
University of Liverpool
176 PUBLICATIONS **2,578** CITATIONS
SEE PROFILE

Klaus Bataille
University of Concepción
87 PUBLICATIONS **1,166** CITATIONS
SEE PROFILE

Tectonophysics 455 (2008) 14–24

Contents lists available at ScienceDirect

Tectonophysics

journal homepage: www.elsevier.com/locate/tecto

First seismic record for intra-arc strike-slip tectonics along the Liquiñe-Ofqui fault zone at the obliquely convergent plate margin of the southern Andes

D. Lange [a,b,*], J. Cembrano [c], A. Rietbrock [d], C. Haberland [e], T. Dahm [b], K. Bataille [f]

[a] University of Potsdam, Institute of Geosciences, Karl-Liebknecht-Straße 24, 14476 Potsdam, Germany
[b] Institute of Geosciences, Bundesstr. 55, 20146 Hamburg, Germany
[c] Universidad Católica del Norte, Avda Angamos 0610, Antofagasta, Chile
[d] University of Liverpool, 4 Brownlow Street, Liverpool L69 3GP, UK
[e] GFZ Potsdam, Telegrafenberg, 14473 Potsdam, Germany
[f] Universidad de Concepción, Casilla 160-C, Concepción, Chile

ARTICLE INFO

Article history:
Received 10 May 2007
Received in revised form 8 April 2008
Accepted 9 April 2008
Available online 22 April 2008

Keywords:
South American Subduction Zone
Southern Chile
Focal mechanisms
Stress partitioning
Strike-slip fault
Liquiñe-Ofqui fault zone

ABSTRACT

A temporal seismic network recorded local seismicity along a 130 km long segment of the transpressional dextral strike-slip Liquiñe-Ofqui fault zone (LOFZ) in southern Chile. Seventy five shallow crustal events with magnitudes up to M_w 3.8 and depths shallower than 25 km were observed in an 11-month period mainly occurring in different clusters. Those clusters are spatially related to the LOFZ, to the volcanoes Chaitén, Michinmahuida and Corcovado, and to active faulting on secondary faults. Further activity along the LOFZ is indicated by individual events located in direct vicinity of the surface expression of the LOFZ. Focal mechanisms were calculated using deviatoric moment tensor inversion of body wave amplitude spectra which mostly yield strike-slip mechanisms indicating a NE–SW direction of the *P*-axis for the LOFZ at this latitude. The seismic activity reveals the present-day activity of the fault zone. The recent M_w 6.2 event near Puerto Aysén, Southern Chile at 45.4°S on April 21, 2007 shows that the LOFZ is also capable of producing large magnitude earthquakes and therefore imposing significant seismic hazard to this region.

1. Introduction

Bulk transpressional deformation is expected at continental margins where the convergence vector is oblique with respect to the plate boundary zone (e.g. Sanderson and Marchini, 1984; Dewey et al., 1998; Fossen and Tikoff, 1998). Kinematic models show that transpressional deformation arising from oblique convergence is accommodated by distinctive structural styles along and across different plate boundaries, which mostly depend on the angle of obliquity, defined as the angle between the convergence vector and the normal to the trench (e.g. Jarrard, 1986a; McCaffrey, 1992). For small angles of obliquity, transpression is homogeneously distributed as in the case of the Australian–Pacific plate boundary in New Zealand (Teyssier et al., 1995). For large angles of obliquity, complete partition of transpression is expected. This is the case of the Pacific–North America plate boundary of the western US, where the San Andreas Fault takes up most of the simple shear components (Teyssier et al., 1995). The general case will be that of heterogeneous transpression in which discrete domains across the plate boundary accommodate wrench-dominated or pure-shear dominated transpression (e.g. Fitch, 1972; Fossen et al., 1994; Tikoff and Greene, 1997). However, the nature and degree of deformation partitioning will not only depend on the angle of obliquity. For instance, thermally weak intra-arc shear zones can accommodate a significant part of the bulk transpressional deformation arising from oblique convergence and affecting the predictions of kinematic models (e.g. De Saint Blanquat et al., 1998). The southern Chilean Andes provides a natural laboratory to examine the nature of long- and short-term transpressional deformation across an obliquely convergent continental margin because of its very well-constrained plate kinematic history. This shows steady right-lateral oblique subduction of the Nazca plate beneath South America since 48 Ma with the exception of nearly orthogonal convergence from 26 to 20 Ma (Pardo-Casas and Molnar, 1987; Somoza, 1998). At present, the angle of obliquity of the Nazca–South America plate convergence vector is, with respect to the orthogonal to the trench normal, approximately 18° for southern Chile (Angermann et al., 1999). The inclination of the Wadati–Benioff zone is about 30° (Haberland et al., 2006; Lange et al., 2007) in southern Chile and the age of the subducting Nazca plate decreases from 30 Ma at 38°S to virtually 0 Ma at 46°S (Müller et al., 1997), where the Chile ridge is currently subducting (e.g. Herron et al., 1981; Cande and Leslie, 1986).

Available structural and thermochronological data documents that the intra-arc Liquiñe-Ofqui fault zone (LOFZ) in the Patagonian Cordillera has accommodated concomitant strike-slip, oblique-slip and reverse-slip ductile to brittle deformation over the last 6 Ma (Hervé et al., 1994; Lavenu and Cembrano, 1999; Cembrano et al., 2002). However, the current deformation state of the arc and the fault

* Corresponding author. Bullard Laboratories, University of Cambridge, Cambridge CB3 0EZ, UK. Tel.: +44 1223 337192; fax: +44 1223 360779.
E-mail address: dl385@cam.ac.uk (D. Lange).

0040-1951/$ – see front matter © 2008 Elsevier B.V. All rights reserved.
doi:10.1016/j.tecto.2008.04.014

zone is still poorly known because of the lack of systematic seismic studies in this remote area of the Andes. A recent event on April 21, 2007 with M_w 6.2 near Puerto Aysén, in the Fjordo Aysén, shows that the LOFZ is also a capable of large magnitude earthquakes and therefore imposes a significant seismic hazard to this region. In this work we present and discuss the first systematic local seismological study of a 130 km long segment of the LOFZ in the Southern Andes between 41.5°S and 43.5°S. Inversion of moment tensors from body waves yield to focal mechanisms which help to constrain the current stress field along the zone. Furthermore, we compare and combine the seismic data with previously published long-term structural data.

2. Structural setting and previous seismic data

The working area (box in Fig. 1) is located in the southern part of the southern volcanic zone (SSVZ) segment (López-Escobar et al., 1993, 1995). The magmatic arc exhibits volcanic activity in the Quaternary (Siebert and Simkin, 2002) and coincides the location of the intra-arc shear zone LOFZ (Cembrano et al., 1996). It had been suggested that the LOFZ controls the location of the larger strato-volcaoes (Stern, 2004, and references therein). This segment of the Andes was part of the proto-Pacific margin of Gondwana and consists of low grade sediments, metabasites, and granitoids which belong to the Patagonian batholith (Pankhurst et al., 1992). The eastern side of the LOFZ had been uplifted and exhumed faster compared to the western side (Adriasola et al., 2006). This kind of margin-parallel strike-slip faults located in magmatic arcs have also been found in other subduction zones with oblique subduction (e.g. Jarrard, 1986b). Based on GPS data Wang et al. (2007) suggest that the LOFZ is the eastern border of a detached continental sliver which moves northward relative to the continent. Evidence for movement of the LOFZ since the Pliocene (Cembrano et al., 1996; Lavenu and Cembrano,

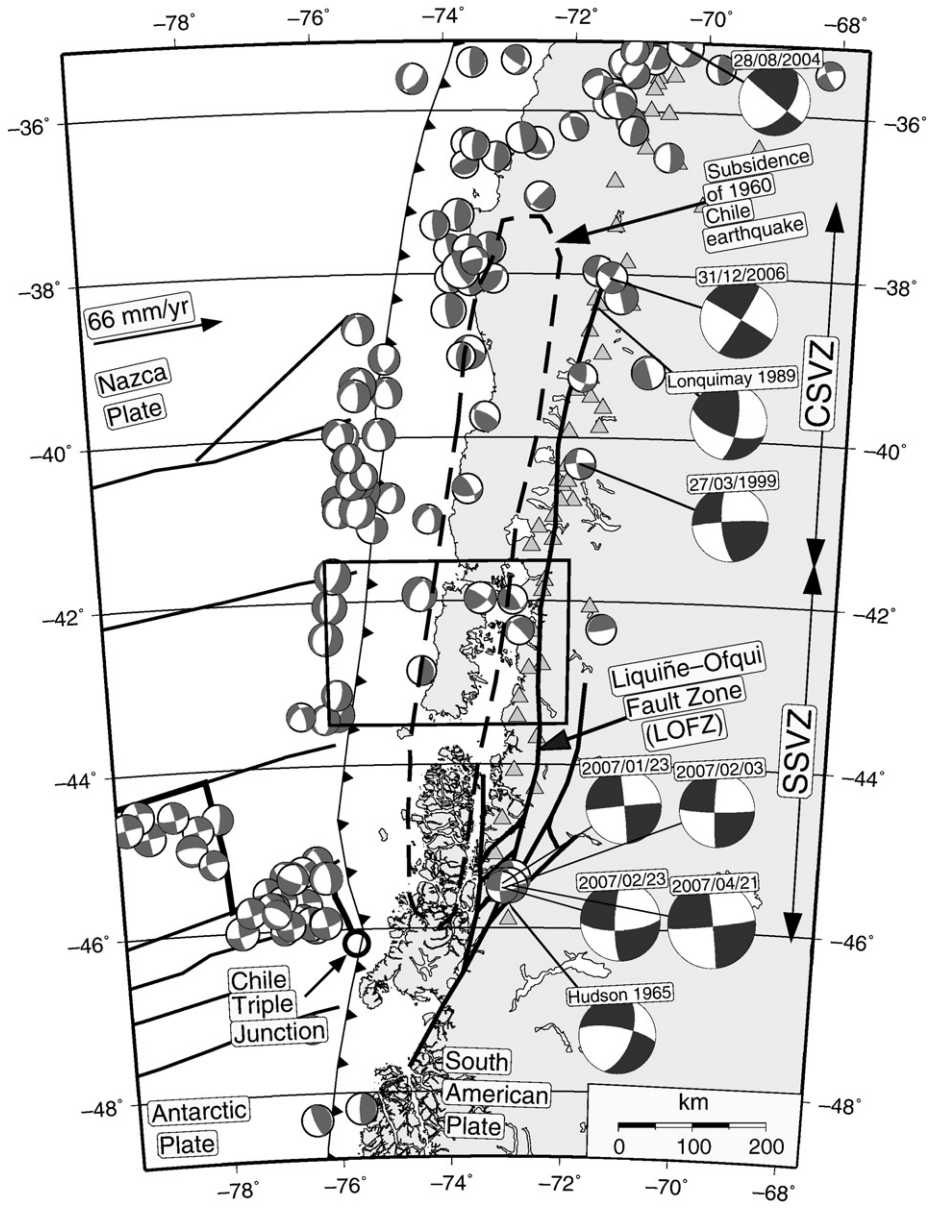

Fig. 1. The southern Andes between 36° and 49°S showing the surface trace of the Liquiñe-Ofqui fault zone (LOFZ), oceanic features and historical focal mechanisms (global CMT catalog). Crustal focal mechanisms attributed to the Liquiñe-Ofqui fault zone (Chinn and Isacks, 1983; Dziewonski et al., 1990) plotted with big circles. The box indicates the location of the seismic network which is plotted in Fig. 2. LOFZ after Cembrano et al. (2000), subsidence of 1960 earthquake after Plafker and Savage (1970). The Nazca–South American plate convergence rate is shown after Angermann et al. (1999). Volcanoes plotted as gray triangles after Siebert and Simkin (2002). Petrographic provinces of the Southern Volcanic zones (SSVZ = Southern Southern Volcanic Zone, CSVZ = Central Southern Volcanic Zone) (López-Escobar et al., 1993, 1995).

1999) is well established. Between 40°S and 42°S latitude complete partitioning of oblique convergence into a margin-normal component (accommodated by the megathrust) and margin-parallel strike-slip component (along the LOFZ) has been proposed by Rosenau et al. (2006).

Crustal seismicity in the magmatic arc is not common for the southern part of the Andes although it exists in the central Andes at 34°S (Barrientos et al., 2004). For the 1000 km long segment of the Andes where the LOFZ is located no significant shallow crustal seismic activity could be observed until now (e.g. Bohm et al., 2002; Rosenau et al., 2006). Nine events of magnitudes between 5.2 and 6.2 (M) have been teleseismically recorded over 40 years along the whole LOFZ (larger focal mechanisms in Fig. 1). However, these earthquake locations have only limited depth accuracy so that the seismicity cannot clearly assigned to the shallower crust. The focal mechanism from Chinn and Isacks (1983) is a 6.0 M_s event which was attributed to an eruption of the Hudson volcano in the year 1965 at 46°S (Rosenau et al., 2006). Another mechanism (5.2 M_w) from Dziewonski et al. (1990) has been associated to the 1989 eruption of the Lonquimay stratovolcano (Barrientos and Acevedo-Aranguiz, 1992). Four recent earthquakes (events 6–9 in Table 1) near Aysén, Southern Chile, with magnitudes between 5.3 and 6.2 (M_w), show that the LOFZ is also capable for producing large magnitude earthquakes and therefore imposing a significant seismic hazard to this region. The teleseismic events are distributed at the northern and southern end of the LOFZ, while for the central segment of the LOFZ no focal mechanisms are available. All teleseismic focal mechanisms show strike-slip movements which are in agreement with the expected N–S right-lateral movement along the LOFZ (if we suppose that the selected fault planes are trending almost N–S). A summary of all teleseismic focal mechanisms is shown in Table 1. North of 38°S, the LOFZ descends in the Antiñir-Copahue fault zone for which Folguera et al. (2004) showed the existence of active faulting. At Lonquimay volcano (38°S), Barrientos and Acevedo-Aranguiz (1992) observed local seismicity after an eruption on December 25, 1988. The events were located beneath the crater of the Lonquimay volcano and did not exceed depths of 10 km. Other local networks along the LOFZ could not observe events located directly on the LOFZ so far (Murdie et al., 1993; Murdie and Russo, 1999; Bohm et al., 2002), or reported only minor seismicity along the LOFZ (Haberland et al., 2006).

Table 1
Summary of historical fault plane solutions for shallow earthquakes along the LOFZ derived from teleseismic observations (Chinn and Isacks, 1983; Dziewonski et al., 1990, 2000) and global CMT catalog

Nr.	Date/time	Lat/Lon	Depth [km] NEIC/CMT	Strike/dip rake	Magnitude (M_w)	Reference
1	1965-11-28	45.77°S	–	20/60	M_s 6.0	Chinn and
	03:56	72.90°W	33	−160	–	Isacks (1983)
2	1989-02-24	39.26°S	–	110/62	5.2	Dziewonski et al. (1990)
	12:36 48.0	71.83°W	15	23	–	Event 129
3	1999-03-27	40.32°S	33	174/72	5.4	Dziewonski et al. (2000)
	11:13 35.6	71.85°W	15	174	–	Event 229
4	2004-08-28	−35.21°S	5	21/61	6.5	CMT
	13:41 35.4	70.36°W	16	−178	–	–
5	2006-12-31	38.04°S	33	031/86	5.5	CMT
	14:55 06.6	71.40°W	12	178	–	–
6	2007-01-23	45.46°S	32	354/89	5.3	CMT
	20:40 15.9	73.07°W	13	−179	–	–
7	2007-02-03	45.51°S	10	091/84	5.3	CMT
	09:00 19.4	73.03°W	12	−6	–	–
8	2007-02-23	45.51°S	25	87/17	5.7	CMT
	19:55 50.1	73.08°W	17	−12	–	–
9	2007-04-21	45.48°S	36	354/88	6.2	CMT
	17:53 48.3	72.95°W	12	176	–	–

3. Data acquisition and analysis

Between December 2004 and November 2005 an amphibious seismic network consisting of 18 land stations and 20 offshore stations was deployed on the island of Chiloé, the corresponding continental region around Chaitén and the offshore forearc between 41.5°S and 43.5°S (Fig. 2). Stations were installed west and east of the LOFZ resulting in a good coverage along the 130 km long segment of the LOFZ between Hornopirén and Chaitén. All landstations were equipped with three-component 1 Hz sensors running in continuous mode with a sample rate of 100 Hz. In total 364 local events were detected on this network during the experiment. They were located utilizing a simultaneous inversion for a one dimensional velocity model, station corrections and hypocenter locations (VELEST program code, Kissling et al. (1994)). Details on the whole network, preprocessing and event location can be found in Lange et al. (2007) and Lange (2008). In this study we focus on the shallow crustal seismicity, including 75 events with focal depths less than 25 km along the LOFZ.

3.1. Inversion of moment tensors

Focal mechanisms were calculated using a deviatoric moment tensor inversion (MTI) approach utilizing the information contained in the observed waveforms. We used amplitude spectra from body waves for selected events with magnitudes between 2.8 and 3.8 (M_w) following the procedure outlined by Dahm et al. (1999) and Cesca et al. (2006). Small earthquakes radiate waves with sufficient signal-to-noise ratio at relatively high frequencies (>0.5 Hz) only. While for larger events moment tensor inversions are nowadays calculated automatically, the determination of reliable MTI for small events is still a challenge. However, MTI were successfully applied to body waves from local events with magnitudes smaller than M_w 4.0 recently (Schurr and Nábělek, 1999; Zahradník et al., 2001; Stich et al., 2003; Cesca et al., 2006; Rößler et al., 2007). Preprocessing prior to MTI includes resampling (20 Hz), restitution of the recorder response, quality control and rotating the traces into the focal coordinate system. Since most of the ocean bottom seismometers are of lesser importance for the local earthquake study here, and have not been calibrated so far, only landstations were used for the MTI. For all given pairs of stations and hypocenter full waveform Green functions (far-field) were calculated (e.g. Cesca et al., 2006) using the 1-D velocity model from Lange et al. (2007). To search for the global minimum in the parameter space a hybrid approach is applied, combining a grid search for different starting parameters and a gradient method to find the minima. The ambiguity of the compressional/tensional sectors is resolved by adding information of first motion polarities of onsets with the highest quality. At least six P-phases and one SH-phase from selected key stations were used for each inversion. Cesca et al. (2006) showed that the azimuthal coverage of the epicenter has a minor impact on the results of the inversion using amplitude spectra tensor inversion which is comparable to the error introduced by wrong velocity models or wrong source time functions. In order to check the stability of the final moment tensors we calculated inversions with different frequency ranges, taper lengths and taper types. The frequency range was restricted between 0.5 and 4.5 Hz (Table 2). Furthermore, we used different source constants (depths/duration) and subsets of stations for the inversion in order to check the appropriate setting of these parameters. The alignment of the synthetic and observed seismograms was checked in the time domain. Some of the events (in particular in the northern part of the study area, see discussion below) exhibit poor azimuthal coverage. However, the small time differences between the P and S arrival times (<1.7 s) at closely located stations clearly indicate that the hypocenters are located in

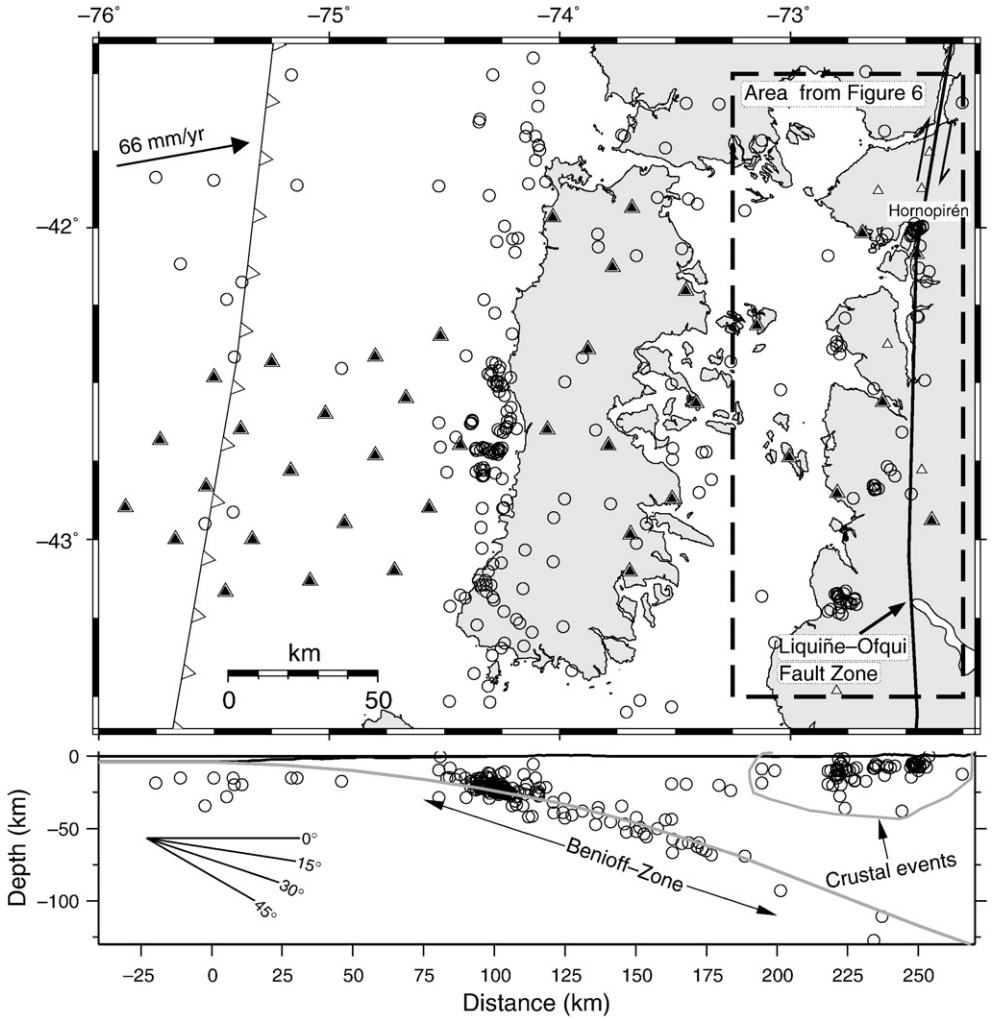

Fig. 2. Top: Station distribution and earthquakes from Lange et al. (2007) used in this study. Seismic stations are indicated with black triangles, volcanoes are indicated by white triangles (Siebert and Simkin, 2002). The Nazca–South American plate convergence rate is shown after Angermann et al. (1999). Bottom: Hypocenters projected onto an E–W vertical cross-section (0.5× vertical exaggeration) clearly show the inclined Wadati–Benioff zone and shallow crustal seismicity. Light gray line indicates interpreted possible top of subducting slab.

the upper crust very close to the next station (Fig. 3). Accordingly, the accurate depths and locations of the events yield a high stability of the MTI. Calculations of Green functions for varying source depths and inversion for the moment tensors for two representative events with magnitudes of 3.0 and 3.2 (M_w) are shown in Fig. 4. The centroid depths calculated by the MTI (using the depth with minimal residual) are comparable with the hypocenter depths derived by the locations derived from the

Table 2
Summary of moment tensor solutions for shallow continental events along the LOFZ

Nr.	Date/time	Lat/Lon	Depth from location routine [km]	Strike/dip rake	DC (%)	Misfit	M0 (dyn*cm)	M_w	f(Hz)	Wave-forms used	Epicentral distance to next stations [km]
1	2005-08-18 18:33 52.4	42.0048°S 72.4387°W	6.86	210/45 −151	88	0.30	7.8E+20	3.2	1.1–4.5	10	6.1/20.5/63.3
2	2005-08-18 21:26 36.5	41.9968°S 72.4393°W	7.43	109/64 −23	83	0.31	5.4E+21	3.76	0.8–4.0	8	10.0/20.6/64.2
3	2005-08-18 21:28 20.3	42.0033°S 72.4515°W	5.90	198/66 169	68	0.29	8.7E+20	3.23	1.0–4.5	8	9.2/19.5/63.3
4	2005-08-22 21:29 05.5	42.0058°S 72.4705°W	6.07	223/22 −120	84	0.19	5.4E+20	3.09	1.0–4.0	10	9.0/17.9/62.7
5	2005-08-23 01:15 21.5	42.0024°S 72.4645°W	6.11	281/66 −4	62	0.22	1.5E+21	3.39	1.1–4.5	8	9.3/18.4/63.2
6	2005-01-18 21:22 29.1	42.3806°S 72.8002°W	10.13	144/45 0	78	0.36	2.13E+20	2.82	1.1–4.5	13	26.0/29.2/41.3
7	2004-12-10 17:03 44.9	42.8437°S 72.6369°W	8.43	231/59 −162	70	0.28	2.7E+21	3.56	0.5–4.0	9	13.1/23.0/31.4
8	2005-05-19 11:44 42.5	42.8001°S 72.5458°W	6.92	319/84 2	62	0.27	3.3E+20	2.95	1.1–4.5	8	20.3/21.3/26.8

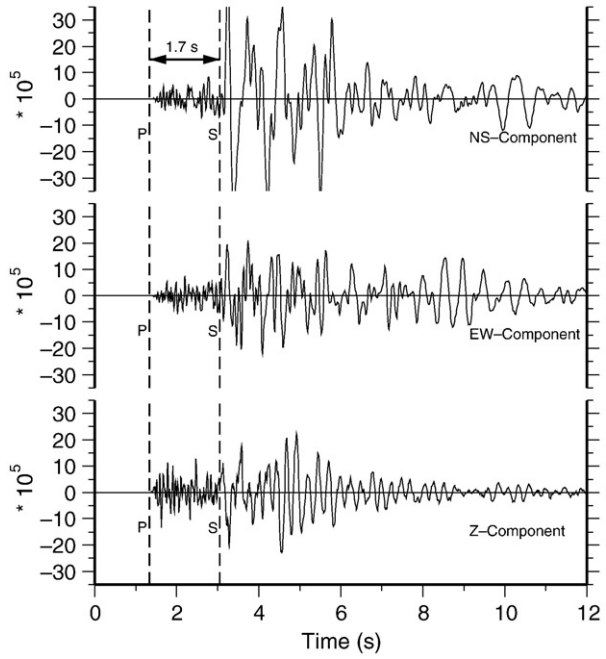

Fig. 3. Example of typical waveforms of the closest station (S15) for onsets arriving from the nearby Hornopirén cluster. The onset of the event from 18.08.2005, 21:26 is shown. P–S time is 1.7 s indicating a short distance to the hypocenter.

arrival times (Lange et al., 2007), differing by less than 1.5 km for all inverted events. These small differences between the hypocentral depth and the depth from the arrival times indicate a small extent of the source region, as suggested by the small magnitudes of the events. Small variations of the depths (±1.5 km) result in only minor variations for strike, dip and rake (±6°). We decomposed the deviatoric part of the moment tensor into a major double-couple and compensated linear vector dipole (CLVD) (Jost and Herrmann, 1989). Since the magnitudes of the inverted events are small, the CLVD is poorly resolved and not considered significant. Synthetic and observed seismograms of amplitude spectra and displacements are shown in Fig. 5 for the M_w 3.2 event at August 18, 2005 (event 2 in Table 2). Because the algorithm only takes into account the far-field radiation, only observations with hypocentral distances bigger than 2 wavelengths (~10 km) were included in the inversion process.

4. Results in discussion

Crustal seismicity in the forearc is clearly separated from the Wadati–Benioff seismicity (Fig. 2). During the 11-month measurement period, 75 events of magnitudes between 0.5 and 3.8 with shallow depths (<25 km) occurred within the continental crust. These events are located in clusters along the LOFZ and can spatially be related to the LOFZ and volcanoes.

In the following we will describe the different cluster in detail from north to south (see also enumeration in Fig. 6):

A.) 10 km south of the small town of Hornopirén (42°S) seismic activity up to magnitude 3.8 (M_w) occurred in a region within the LOFZ (Fig. 7). The main events, which were felt by the inhabitants of Hornopirén, occurred at 18/08/2005, 21:26 and 21:28 (M_w 3.8 and 3.2) followed by events 22/08/2005, 21:29 and 23/08/2005, 01:15 with M_w of 3.1 and 3.4, respectively. In total, we detected 32

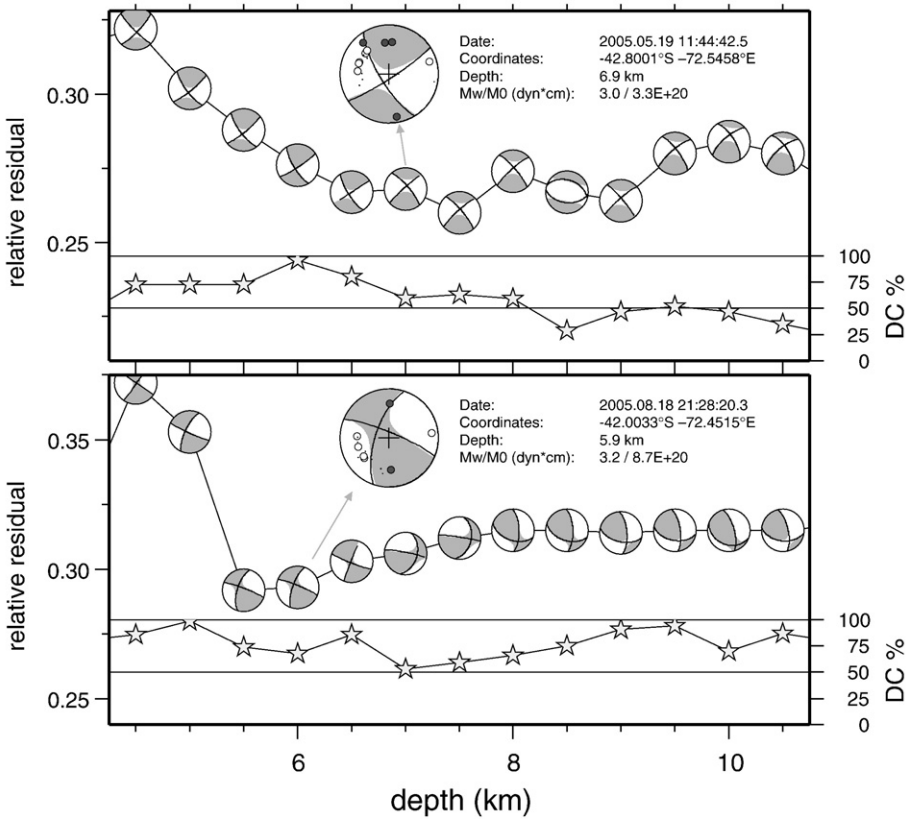

Fig. 4. Summary of the inversion for two representative events. Inverted focal mechanisms and double-couple moment tensor components plotted versus varying depths. The final solution (the solution with the depth from the inversion routine) for the two events is plotted with high quality first motion polarities and marked with an arrow. Double couple components plotted as stars.

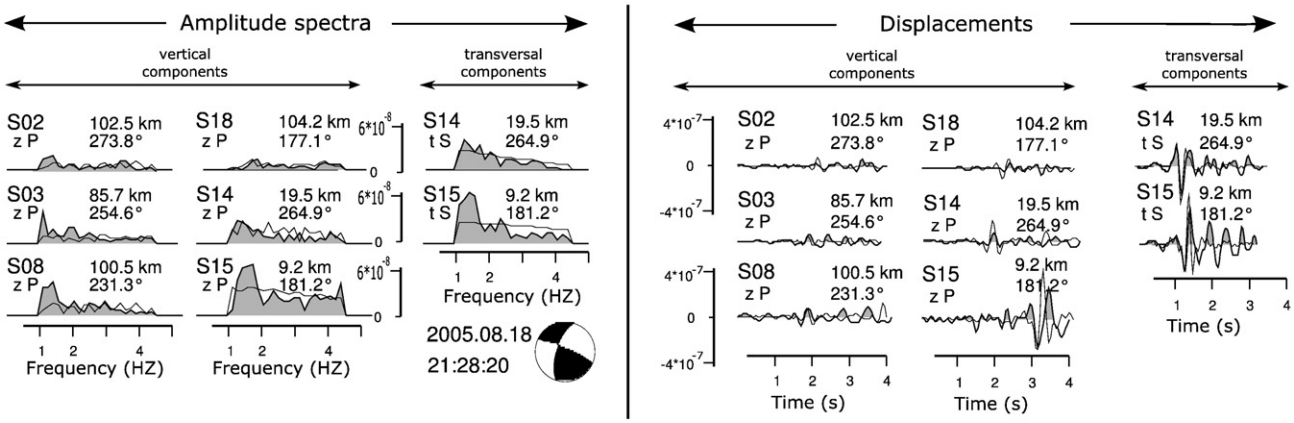

Fig. 5. Comparison between synthetic (lines) and observed (gray areas) amplitude spectra for vertical components (P-phase, zP) and transversal components (S-phase, tS). The event (M_w 3.2) occurred on August 18, 2005 21:28 UTC. The components are annotated with station name, distance, backazimuth and phase. The displacements were calculated using the time domain inversion of the programme MTINVERS. Amplitude spectra and displacements are plotted with the same scale each.

events in 5 days from this cluster, from which 19 events reveal more then 8 P and 4 S readings. The distances from this seismicity cluster to the three nearest stations were 10, 20 and 60 km, respectively. The events are located at shallow depths between 5 and 8 km (Fig. 7). Most of the focal mechanisms (events 1–5 in Table 2) exhibit a similar strike-slip characteristic (Fig. 7). The possible activated fault planes on which the movement occurred are trending ~10° or ~100°. The observed events reside on the eastern branch of NNE–SSW trending faults bounding a pull-apart basin (Dewey and Lamb, 1992). Taking into account both the NS trending surface expression of the LOFZ (~10°N) and the predominantly NS-striking dextral strike-slip mesoscopic faults seen along this fault trace (Cembrano et al., 2000), NS oriented strike-slip movement is most likely, resulting in a dextral strike-slip fault plane inline with the regional geological observations. The smallest magnitude event from this cluster (M_w 3.1) is the only event which does not reveal strike-slip mechanism indicating extension. This focal mechanism is nicely consistent with the NW-trending extension axis as resulting from a broad, NS-striking, dextral shear zone, however one mechanism is difficult to interpret. The deepest event with a depth of 7.6 km inside the LOFZ near Hornopirén (Fig. 7) gives a minimum depth extent of ~8 km for the LOFZ at this latitude. The location of the cluster directly below the surface trace of the LOFZ, described by Cembrano et al. (2000) in Fig. 7, indicates a relatively steep inclination of the fault system. Because the distance from this cluster to the Hornopirén volcano is 20 km (Fig. 6), we suggest that this cluster is related to the LOFZ and not directly related to activity of the volcano Hornopirén, indicating current activity of the fault zone. Further activity along the LOFZ is indicated by individual events located in direct vicinity of the LOFZ more to the south (Fig. 6), with distances to the adjacent volcanoes of up to 30 km.

B.) Along the south western coast of Huequi peninsula five events occurred. The Huequi volcanoes in the center of the island erupted in 1906 explosively (Casertano, 1963). The focal mechanism for the strongest event in this cluster (M_w 2.8) is strike-slip . We suggest that this cluster is related to a ~135° (±15°) trending fault which forms the coast line and continues to the South into the valley SE of station S16 (see Fig. 8). The seismicity cluster is located 15 km west from the Huequi volcano, suggesting that these events are not directly activity-related to the volcano.

C.) Below Chaitén volcano, a postglacial caldera or explosion crater, 3 km in diameter (López-Escobar et al., 1993), we observed seismicity up to M_w 3.6. Naranjo and Stern (2004) dated the last eruption of Chaitén volcano at 9370 BP. Chaitén caldera is developed along a 14 km SW–NE oriented fissure (López-Escobar et al., 1995), in the direction of the greatest compressional horizontal stress. Main seismicity in this area is spatially related to the Chaitén caldera located on the western flank of Michinmahuida, a stratovolcano with a permanent ice cap. The two focal mechanisms for this cluster again show strike-slip mechanisms with 40° or 130° strike direction of the two possible fault planes. The event on Mai 19, 2005 is the south-easternmost event of NW–SE aligned hypocenters (Figs. 6 and 8). Accordingly, we relate this event to a NW–SE trending fault plane.

D.) The southernmost cluster of seismicity is found around the Corcovado volcano. Compared to the other clusters the hypocentral resolution is much lower because the events are all outside the network. Nevertheless, this cluster has strong activity in terms of event number, but the magnitude of the events does not exceed M_w 2.6. Because of the poor azimuthal coverage a reliable moment tensor solution could not be obtained for the events in this cluster.

For the inversion of the stress field we applied the method from Michael (1984, 1987). The inverted stress tensor is compatible with the deformation field derived from both kinematic analysis of Pliocene mylonites and inversion of Pleistocene fault-slip data which consistently yield a long-term greatest compressional stress axis oriented northeast (Lavenu and Cembrano, 1999; Cembrano et al., 2000), indicating a stable tectonic regime along the fault zone at this latitude (Fig. 9). Furthermore, the 60° striking elongation of the volcanoes (Nakamura, 1977; Rosenau et al., 2006) is close to the trending of σ_1 from actual seismicity and the mylonitic faults. Since a direction of 55° of σ_1 for a 10°E trending strike-slip deformation zone is the expected shortening axis (López-Escobar et al., 1995), the N76E-trending σ_1 as derived from the stress field inversion is consistent with tectonic models of slip partitioning across obliquely convergent margins (e.g. Fitch, 1972; Beck, 1983).

Different factors suggest a tectonic or volcano-tectonic origin of the observed seismicity. Events below Corcovado and Chaitén volcanoes (cluster C and D) exhibit P and S onsets; during the 11 month

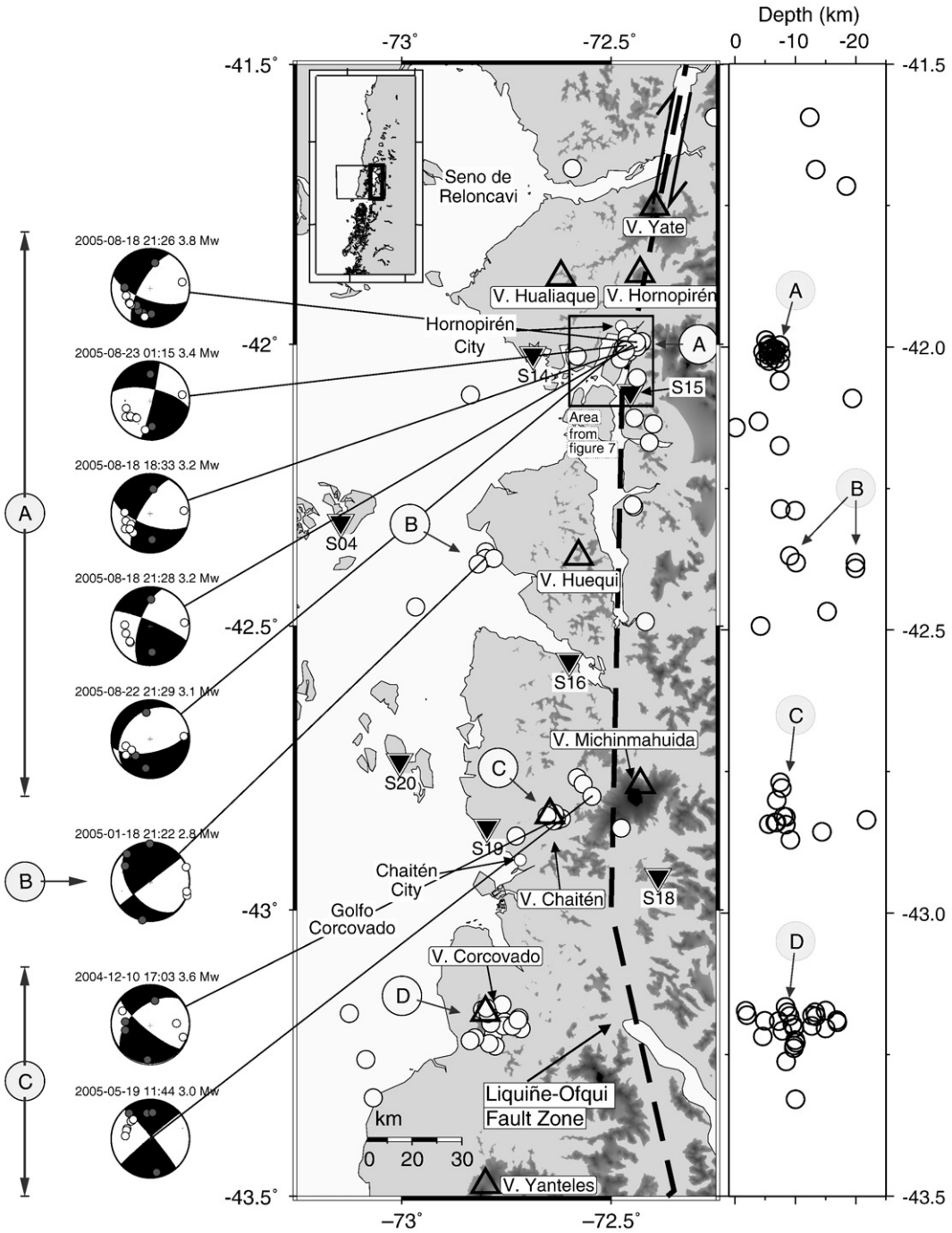

Fig. 6. Crustal seismicity with MTI solutions (double-couple component, lower hemisphere plot with polarities of high quality) along the LOFZ between 41.5°S and 43.5°S is located in four clusters (A–D). Seismic stations are indicated by inverted triangles. Volcanoes are indicated with upright triangles (Siebert and Simkin, 2002). Box indicates the location of the close-up view shown in Fig. 7.

observation period no volcanic tremor-like signals were observed like those further north at Villarrica volcano (e.g. Ortiz et al., 2003). Furthermore, MTI solutions for the whole moment tensor (six components) do not show elevated isotropic moment tensor components, but indicate predominantly double-couple mechanisms. The similarity of the two independently derived solutions for long- and short-term deformation suggests that the stress regime has been stable since the Pliocene. Strike-slip faults occur in about 50% of modern subduction zones (Jarrard, 1986b). The model of slip partitioning due to oblique subduction is applied to many of them e.g. the Great Sumatran Fault (Beck, 1983; Baroux et al., 1998; McCaffrey et al., 2000) and others (Jarrard, 1986b; Kimura, 1986). Like the LOFZ many of these fault zones are accompanied by volcanic arcs. McCaffrey et al. (2000) observed for the Sumatra fault that two thirds of the margin-parallel component of relative plate motion occurs on the Sumatran strike-slip fault, the rest occurred near the trench. It has been proposed that for the southern Chilean margin the actual obliquity is too small to account by itself for strike-slip tectonics (Cembrano et al., 2000). For the southern Chilean Andes it is suggested that the key factors for intra-arc faulting are a thermally weak continental crust and strong intraplate coupling (Cembrano et al., 2000) and/or the active

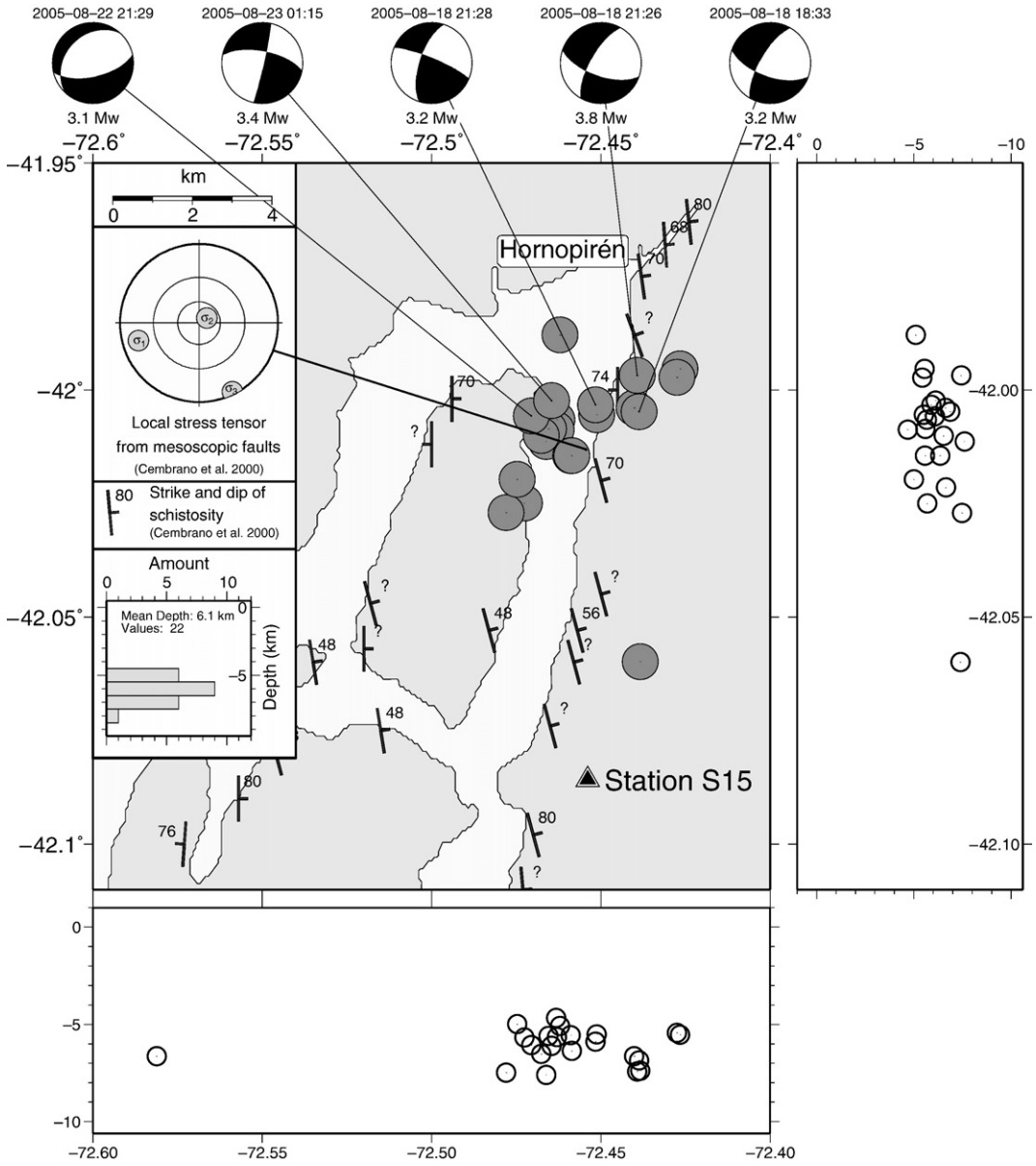

Fig. 7. Blow-up view (16×16 km) of the events near Hornopirén (cluster A in Fig. 6) with corresponding focal mechanisms (double-couple). The local stress tensor of Cembrano et al. (2000), derived from mesoscopic faults, is plotted in the inlay (stereographic, lower hemisphere projection) and shows a strike-slip stress regime. A NW-striking mylonitic foliation, along with a subhorizontal stretching lineation are observed along and across the NNE-striking, approximately 4 km wide, ductile shear zone representing the LOFZ. This shear zone records Pliocene dextral strike-slip deformation (Cembrano et al., 2000). All of the hypocenters have depths of less than 10 km (see depth profiles) below surface outcrops of the LOFZ indicating a steep inclination of the fault zone. The closest seismic station (S15) is indicated by a black triangle. Location of close-up-view is indicated in Fig. 6.

subduction of the Chile Ridge indenter at the trailing edge of the LOFZ (Forsythe and Nelson, 1985; Cembrano et al., 2002).

5. Conclusions

With our temporary seismic network we detected seismicity with magnitudes up to 3.8 (M_w) occurring in several distinct spatial clusters along the LOFZ and the volcanic arc. The clusters are spatially distinct with one occurring below the surface expression of the LOFZ and two beneath volcanoes. The main cluster of seismicity is located below the surface trace of the LOFZ indicating the ongoing activity at this prominent intra-arc shear zone. Focal mechanisms derived from teleseismic and local data show similar strike-slip mechanisms for the whole LOFZ. The location and the strike-slip mechanism of events in two clusters suggest that NW–SE trending secondary faults are currently active (Fig. 8). It is likely these faults are not actually connected nor genetically related to the LOFZ. They are long-lived basement structures that cross the LOFZ from the Argentinian foreland. In fact, some of these NW lineaments have cut and displaced segments of the LOFZ with a sinistral strike-slip sense. Strike-slip mechanisms support the hypothesis of slip partitioning due to oblique subduction (Beck et al., 1993) or ridge subduction (Nelson et al., 1994). The observed dextral deformation along the LOFZ is inline with the proposed northward movement of a forearc sliver acting as a detached continental micro-plate as outlined by Forsythe and Nelson (1985) and Beck et al. (1993) (Fig. 10). Based on GPS data Wang et al. (2007) modeled the sliver motion as a northward directed block translation at a rate of 6.5 mm/yr (30% of the relative

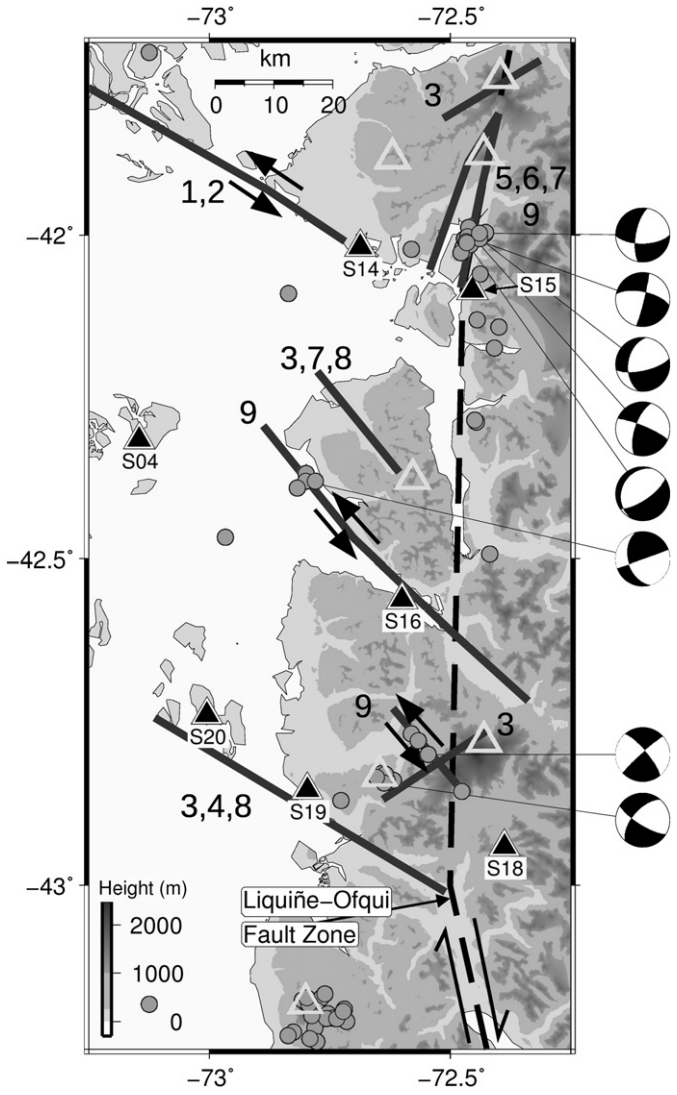

Fig. 8. Compilation of major faults and alignments along the LOFZ (between 41.5°S and 43.5°S) and crustal seismicity with focal mechanisms. Seismic stations are black triangles, volcanoes are indicated with unfilled triangles. Numbers indicate references of faults and alignments: 1: Melnick and Echtler (2006), 2: Hackney et al. (2006), 3: López-Escobar et al. (1995), 4: Lavenu and Cembrano (1999), 5: Cembrano et al. (2000), 6: Dewey and Lamb (1992), 7: Sernageomin (2003), 8: Cembrano et al. (1996) 9: This study.

margin-parallel convergence velocity), with the rate tapering to zero at the northern termination of the LOFZ. The existence of an north ward moving forearc sliver cannot be settled conclusively with the actual data, but it is currently the most plausible explanation. To confirm this model additional geodetic and geological data is needed, especially a dense GPS network in the vicinity of the LOFZ. Because the LOFZ is located far east of the surface projection of the coupled plate interface, the existence of a forearc sliver would raise the question of its deep structure. The recent activity of the LOFZ revealed by local seismicity, together with the recent strong event (6.2 M_w) from April 21, 2007 at the southern part of the LOFZ, should be taken into account for future hazard analysis.

Acknowledgements

The TIPTEQ seismic array was run collaboratively by the University of Potsdam (Germany), University of Hamburg (Germany), University of Liverpool (UK), the Universidad de Concepción (Chile) and the IFM-GEOMAR (Germany). We gratefully acknowledge the cooperation of many Chilean landowners, companies, and institutions for support and for allowing us to install seismic stations on their property. In particular we are grateful to the Administration of Parque Pumalin for the permission to deploy the station in Caleta Gonzalo and to the Empresa Fjordo Blanco for permission to deploy the station on the Island of Talcan and for support. Furthermore, we thank all field crews for their excellent work under difficult conditions, especially G. Hermosilla, M. Piña, M. Moreno, J. Jarra, F. Sanchez, V. Venegas and M. Contreras.

GIPP (GFZ) and IFM-GEOMAR provided instruments. We would like to thank Frank Krüger, Dirk Rößler, Barbara Hofmann, Daniel Melnick and Matt Miller for their constructive comments and suggestions. We thank the master and crew of R/V SONNE cruise SO 181 for the deployment of the OBS/OBH. All figures were generated using GMT (Wessel and Smith, 1998). This is publication no. GEOTECH-227 of the R&D Programme GEOTECHNOLOGIEN funded by the German Ministry of Education and Research (BMBF) and German Research Foundation (DFG), grant 03G0594C. JC acknowledges Fondecyt project 1060187 on the interplay between tectonics and volcanism in the southern Andes. We also thank Raul

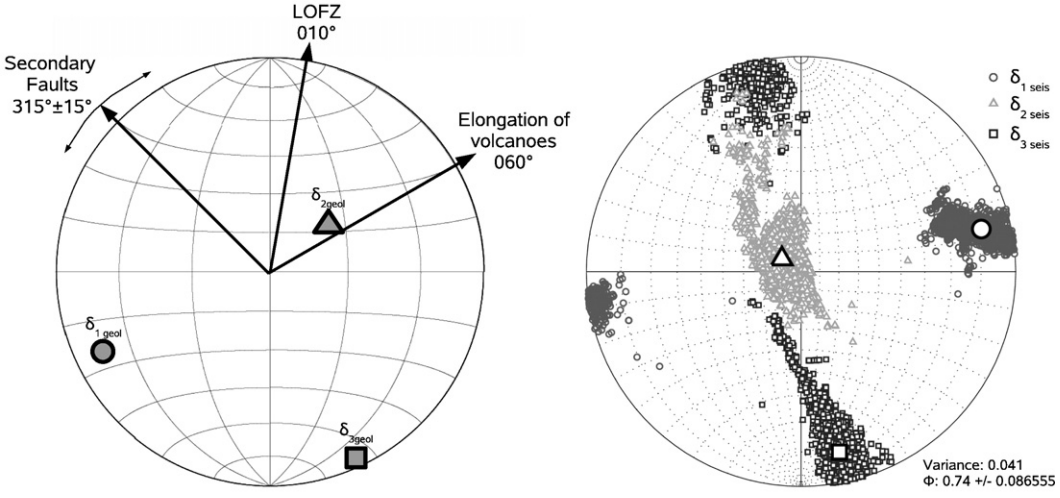

Fig. 9. Lower hemisphere, equal area projections showing the orientation of the stress tensors from faults and acutal seismicity. Left: Projection showing the orientation of the local stress tensor of mesoscopic faults (σ_{geol}) from Cembrano et al. (2000) together with the orientation of faults and elongated volcanoes. Right: Projection showing the result of stress tensor inversion (Michael, 1984, 1987) of the continental events along the LOFZ (Fig. 6). The stress tensor exhibits a strike-slip regime with 76° trending of σ_1. The small symbols indicate the results of the bootstrap calculations.

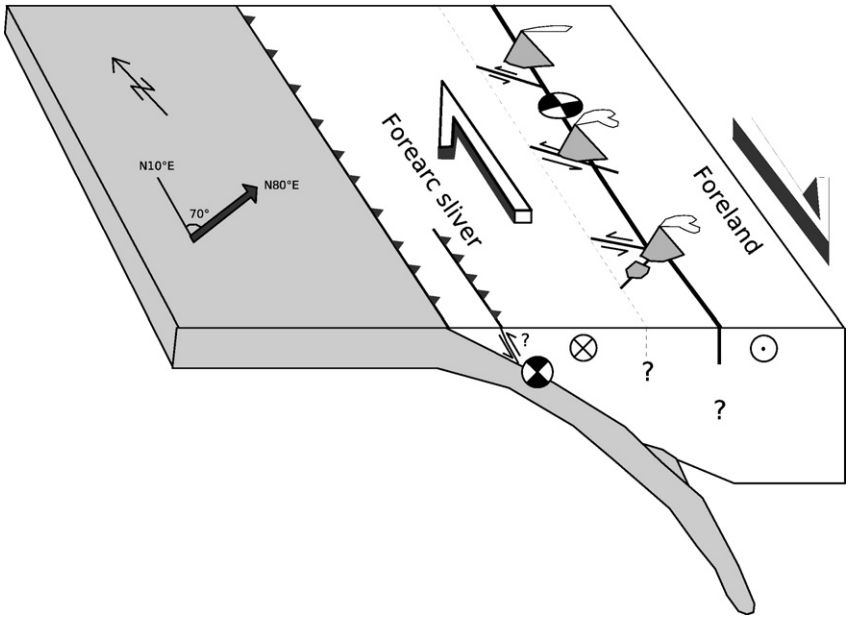

Fig. 10. Proposed tectonic model for southern Chile. Partitioning of the oblique convergence vector between the Nazca plate and South American plate results in a dextral strike-slip fault zone in the magmatic arc and a northward moving forearc sliver. Modified after Lavenu and Cembrano (1999).

Madariaga and Denis Legrand for helpful comments and constructive suggestions.

References

Adriasola, A., Thomson, S., Brix, M., Hervé, F., Stöckhert, B., 2006. Postmagmatic cooling and late Cenozoic denudation of the North Patagonian Batholith in the Los Lagos region of Chile, 41°–42°15'S. Int. J. Earth Sci. 95 (3), 504–528.

Angermann, D., Klotz, J., Reigber, C., 1999. Space-geodetic estimation of the Nazca–South America Euler vector. Earth Planet. Sci. Lett. 171 (3), 329–334.

Baroux, E., Avouac, J.-P., Bellier, O., Sébrier, M., 1998. Slip-partitioning and fore-arc deformation at the Sunda Trench, Indonesia. Terra Nova 10 (3), 139–144.

Barrientos, S.E., Acevedo-Aranguiz, P.S., 1992. Seismological aspects of the 1988–1989 Lonquimay (Chile) volcanic eruption. J. Volcanol. Geotherm. Res 53 (1-4), 73–87.

Barrientos, S., Vera, E., Alvarado, P., Monfret, T., 2004. Crustal seismicity in central Chile. J. South Am. Earth Sci. 16 (8), 759–768.

Beck Jr., M.E., 1983. On the mechanism of tectonic transport in zones of oblique subduction. Tectonophysics 93 (1-2), 1–11.

Beck Jr., M.E., Rojas, C., Cembrano, J., 1993. On the nature of buttressing in margin-parallel strike-slip fault systems. Geology 21 (8), 755–758.

Bohm, M., Lüth, S., Echtler, H., Asch, G., Bataille, K., Bruhn, C., Rietbrock, A., Wigger, P., 2002. The Southern Andes between 36°and 40°S latitude: seismicity and average seismic velocities. Tectonophysics 356 (4), 275–289.

Cande, S.C., Leslie, R.B., 1986. Late Cenozoic tectonics of the southern Chile Trench. J. Geophys. Res. 91 (B1), 471–496.

Casertano, L., 1963. General characteristics of active Andean volcanoes and a summary of their activities during recent centuries. Bull. Seismol. Soc. Am. 53 (6), 60–631.

Cembrano, J., Hervé, F., Lavenu, A., 1996. The Liquiñe Ofqui fault zone: a long-lived intra-arc fault system in southern Chile. Tectonophysics 259, 55–66.

Cembrano, J., Schermer, E., Lavenu, A., Sanhueza, A., 2000. Contrasting nature of deformation along an intra-arc shear zone, the Liquiñe-Ofqui fault zone, southern Chilean Andes. Tectonophysics 319, 129–149.

Cembrano, J., Lavenu, A., Reynolds, P., Arancibia, G., López, G., Sanhueza, A., 2002. Late Cenozoic transpressional ductile deformation north of the Nazca–South America–Antarctica triple junction. Tectonophysics 354 (3-4), 289–314.

Cesca, S., Buforn, E., Dahm, T., 2006. Amplitude spectra moment tensor inversion of shallow earthquakes in Spain. Geophys. J. Int. 166 (2), 839–854. doi:10.1111/j.1365-246X.2006.03073.x.

Chinn, D.S., Isacks, B.L., 1983. Accurate source depths and focal mechanisms of shallow earthquakes in western South America and in the New Hebrides island arc. Tectonics 2 (6), 529–563.

Dahm, T., Manthei, G., Eisenblätter, J., 1999. Automated moment tensor inversion to estimate source mechanisms of hydraulically induced micro-seismicity in salt rock. Tectonophysics 306 (1), 1–17.

De Saint Blanquat, M., Tikoff, B., Teyssier, C., Vigneresse, J.L., 1998. Transpressional kinematics and magmatic arcs. Spec. Publ. - Geol. Soc. 135, 327–340.

Dewey, J.F., Lamb, S.H., 1992. Active tectonics of the Andes. Tectonophysics 205 (1-3), 79–95.

Dewey, J.F., Holdsworth, R.E., Strachan, R.A., 1998. Transpression and transtension zones. Spec. Publ. - Geol. Soc. 135, 1–14.

Dziewonski, A.M., Ekström, G., Woodhouse, J.H., Zwart, G., 1990. Centroid-moment tensor solutions for January–March 1989. Phys. Earth Planet. Inter. 59 (4), 233–242.

Dziewonski, A.M., Ekström, G., Maternovskaya, N.N., 2000. Centroid-moment tensor solutions for January–March 1999. Phys. Earth Planet. Inter. 118, 1–11.

Fitch, T.J., 1972. Plate convergence, transcurrent faults, and internal deformation adjacent to Southeast Asia and the Western Pacific. J. Geophys. Res. 77, 4.432–4.461.

Folguera, A., Ramos, V.A., Hermanns, R.L., Naranjo, J., 2004. Neotectonics in the foothills of the southernmost central Andes (37°–38°S): evidence of strike-slip displacement along the Antiñir-Copahue fault zone. Tectonics 23 (5), 541–566.

Forsythe, R., Nelson, E., 1985. Geological manifestations of ridge collision: evidence from the Golfo de Penas–Taitao basin, southern Chile. Tectonics 4 (5), 477–495.

Fossen, H., Tikoff, B., 1998. Extended models of transpression and transtension, and application to tectonic settings. Spec. Publ. - Geol. Soc. 135, 15–33.

Fossen, H., Tikoff, B., Teyssier, C., 1994. Strain modeling of transpressional and transtensional deformation. Norsk Geologisk Tidsskrift 74 (3), 134–145.

Haberland, C., Rietbrock, A., Lange, D., Bataille, K., Hofmann, S., 2006. Interaction between forearc and oceanic plate at the south-central Chilean margin as seen in local seismic data. Geophys. Res. Lett. 33, L233023. doi:10.1029/2006GL028189.

Hackney, R., Echtler, H., Franz, G., Götze, H.-J., Lucassen, F., Marchenko, D., Melnick, D., Meyer, U., Schmidt, S., Tášrová, Z., Tassara, A., Wienecke, S., 2006. The segmented overriding plate and coupling at the south-central Chilean margin (36° and 42°S). In: Oncken, O., Chong, G., Franz, G., Giese, P., Götze, H.-J., Ramos, V.A., Strecker, M., Wigger, P. (Eds.), The Andes — Active Subduction Orogeny. Springer, pp. 355–374. doi:10.1007/978-3-540-48684-8_17.

Herron, E.M., Cande, S.C., Hall, B.R., 1981. An active spreading center collides with a subduction zone: a geophysical survey of the Chile margin triple junction. Geol. Soc. Am. Mem. 154, 683–701.

Hervé, F., Greene, F., Pankhurst, R.J., 1994. Metamorphosed fragments of oceanic crust in the Upper Paleozoic Chonos accretionary complex, southern Chile. J. South Am. Earth Sci. 7 (3-4), 263–270.

Jarrard, R.D., 1986a. Relations among subduction parameters. Rev. Geophys. 24 (2), 217–284.

Jarrard, R.D., 1986b. Terrane motion by strike-slip faulting of forearc slivers. Geology 14 (9), 780–783.

Jost, M., Herrmann, R., 1989. A student's guide to and review of moment tensors. Seismol. Res. Lett. 60, 37–57.

Kimura, G., 1986. Oblique subduction and collision: forearc tectonics of the Kuril arc. Geology 14 (5), 404–407.

Kissling, E., Ellsworth, W.L., Eberhart-P hillips, D., Kradolfer, U., 1994. Initial reference models in local earthquake tomography. J. Geophys. Res. 99 (B10), 19.635–19.646.

Lange, D., 2008. The South Chilean Subduction Zone between 41°S and 43.5°S: Seismicity, Structure and State of Stress. Ph.D. thesis, University of Potsdam.

Lange, D., Rietbrock, A., Haberland, C., Bataille, K., Dahm, T., Tilmann, F., Flüh, E., 2007. Seismicity and geometry of the south Chilean subduction zone (41.5°S–43.5°S): implications for controlling parameters. Geophys. Res. Lett. 34, L06311. doi:10.1029/2006GL029190.

Lavenu, A., Cembrano, J., 1999. Compressional- and transpressional-stress pattern for Pliocene and Quaternary brittle deformation in fore arc and intra-arc zones (Andes of Central and Southern Chile). J. Struct. Geol. 21 (12), 1.669–1.691.

López-Escobar, L., Kilian, R., Kempton, P.D., Tagiri, M., 1993. Petrography and geochemistry of Quaternary rocks from the Southern Volcanic Zone of the Andes between 41° and 46°S, Chile. Rev. Geol. Chile 20 (1), 33–55.
López-Escobar, L., Cembrano, J., Moreno, H., 1995. Geochemistry and tectonics of the Chilean Southern Andes basaltic Quaternary volcanism (37–46°S). Rev. Geol. Chile 22 (2), 219–234.
McCaffrey, R., 1992. Oblique plate convergence, slip vectors, and forearc deformation. J. Geophys. Res. 97 (B6), 8.905–8.915.
McCaffrey, R., Zwick, P.C., Bock, Y., Prawirodirdjo, L., Genrich, J.F., Stevens, C.W., Puntodewo, S.S.O., Subarya, C., 2000. Strain partitioning during oblique plate convergence in northern Sumatra: geodetic and seismologic constraints and numerical modeling. J. Geophys. Res. 105 (B12), 28.363–28.376.
Melnick, D., Echtler, H., 2006. Morphotectonic and geologic digital map compilations of the South-Central Andes (36°–42°S). In: Oncken, O., Chong, G., Franz, G., Giese, P., Götze, H.-J., Ramos, V.A., Strecker, M., Wigger, P. (Eds.), The Andes — Active Subduction Orogeny. Springer, pp. 565–568. doi:10.1007/978-3-540-48684-8_30.
Michael, A.J., 1984. Determination of stress from slip data: faults and folds. J. Geophys. Res. 89 (B13) 11.517–11.526. 544.
Michael, A.J., 1987. Use of focal mechanisms to determine stress: a control study. J. Geophys. Res. 92 (B1), 357–369.
Müller, R.D., Roest, W.R., Royer, J.-Y., Gahagan, L.M., Sclater, J.G., 1997. Digital isochrons of the world's ocean floor. J. Geophys. Res. 102 (B2), 3211–3214 ftp://ftp.es.usyd.edu.au/pub/agegrid/.
Murdie, R.E., Russo, R.M., 1999. Seismic anisotropy in the region of the Chile margin triple junction. J. South Am. Earth Sci. 12 (3), 261–270.
Murdie, R.E., Prior, D.J., Styles, P., Flint, S.S., Pearce, R.G., Agar, S.M., 1993. Seismic responses to ridge-transform subduction: Chile triple junction. Geology 21 (12), 1.095–1.098.
Nakamura, K., 1977. Volcanoes as possible indicators of tectonic stress orientation — principle and proposal. J. Volcanol. Geotherm. Res. 2, 1–16.
Naranjo, J.A., Stern, C.R., 2004. Holocene tephrochronology of the southernmost part (42°30'–45°S) of the Andean Southern Volcanic Zone. Rev. Geol. Chile 31 (2), 225–240.
Nelson, E., Forsythe, R., Arit, I., 1994. Ridge collision tectonics in terrane development. J. South Am. Earth Sci. 7 (3-4), 271–278.
Ortiz, R., Moreno, H., García, A., Fuentealba, G., Astiz, M., Peña, P., Sánch ez, N., Tárraga, M., 2003. Villarrica volcano (Chile): characteristics of the volcanic tremor and forecasting of small explosions by means of a material failure method. J. Volcanol. Geother. Res. 128, 247–259.
Pankhurst, R.J., Herve, F., Rojas, L., Cembrano, J., 1992. Magmatism and tectonics in continental Chiloé, Chile (42°–42°30'S). Tectonophysics 205 (1-3), 283–294.
Pardo-Casas, F., Molnar, P., 1987. Relative motion of the Nazca (Farallon) and South American plates since late Cretaceous time. Tectonics 6 (3), 233–248.
Plafker, G., Savage, J.C., 1970. Mechanism of the Chilean Earthquakes of May 21 and 22, 1960. Geol. Soc. Am. Bull. 81, 1.001–1.030.
Rosenau, M., Melnick, D., Echtler, H., 2006. Kinematic constraints on intra-arc shear and strain partitioning in the Southern Andes between 38°S and 42°S latitude. Tectonics 25, TC4013. doi:10.1029/2005TC001943.
Rößler, D., Krüger, F., Rümpker, G., 2007. Retrieval of moment tensors due to dislocation point sources in anisotropic media using standard techniques. Geophys. J. Int. 169, 136–148. doi:10.1111/j.1365-246X.2006.03243.x.
Sanderson, D.J., Marchini, W.R.D., 1984. Transpression. J. Struct. Geol. 6 (5), 449–458.
Schurr, B., Nábělek, J., 1999. New techniques for the analysis of earthquake sources from local array data with an application to the 1993 Scotts Mills, Oregon aftershock sequence. Geophys. J. Int. 137, 585–600.
Sernageomin (2003). Mapa Geológico de Chile: versión digital, N°4, CD-ROM, versión 1.0. Servicio Nacional de Geología y Minería, Publicación Geológica Digital, Santiago, Chile.
Siebert, L., Simkin, T., (2002). Volcanoes of the World: An Illustrated Catalog of Holocene Volcanoes and their Eruptions. Smithsonian Institution, Global Volcanism Program Digital Information Series. GVP-3. http://www.volcano.si.edu/world/.
Somoza, R., 1998. Updated Nazca (Farallon)–South America relative motions during the last 40 My: implications for mountain building in the central Andean region. J. South Am. Earth Sci. 11 (3), 211–215.
Stern, C.R., 2004. Active Andean volcanism: its geologic and tectonic setting. Rev. Geol. Chile 31 (2), 161–206.
Stich, D., Ammon, C.J., Morales, J., 2003. Moment tensor solutions for small and moderate earthquakes in the Ibero-Maghreb region. J. Geophys. Res. 108 (B3), 2148. doi:10.1029/2002JB002057.
Teyssier, C., Tikoff, B., Markley, M., 1995. Oblique plate motion and continental tectonics. Geology 23 (5), 447–450.
Tikoff, B., Greene, D., 1997. Stretching lineations in transpressional shear zones: an example from the Sierra Nevada Batholith, California. J. Struct. Geol. 19 (1), 29–39.
Wang, K., Hu, Y., Bevis, M., Kendrick, E., Smalley Jr., R., Vargas, R.B., Lauría, E., 2007. Crustal motion in the zone of the 1960 Chile earthquake: detangling earthquake-cycle deformation and forearc-sliver translation. Geochem. Geophys. Geosyst. 8. doi:10.1029/2007GC001721.
Wessel, P., Smith, W.H.F., 1998. New, improved version of the Generic Mapping Tools released. suppl. to EOS, Transactions. AGU 79, 579.
Zahradník, J., Janský, J., Papatsimpa, K., 2001. Focal mechanisms of weak earthquakes from amplitude spectra and polarities. Pure Appl. Geophys. 158 (4), 647–665.